

Characterization of the human platelet N- and O-glycome upon storage using tandem mass spectrometry

Katelyn E. Rosenbalm,¹ Melissa M. Lee-Sundlov,¹ David J. Ashline,² Renata Grozovsky,³ Kazuhiro Aoki,^{4,5} Andrew J. S. Hanneman,^{1,6} and Karin M. Hoffmeister¹

¹Translational Glycomics Center, Versiti Blood Research Institute, Milwaukee, WI; ²The Glycomics Center, Division of Molecular, Cellular and Biomedical Sciences, University of New Hampshire, Durham, NH; ³Department of Otolaryngology, University of Miami Miller School of Medicine, Miami, FL; ⁴Department of Cell Biology, Neurobiology and Anatomy, Medical College of Wisconsin, Milwaukee, WI; ⁵Medical College of Wisconsin Cancer Center, Milwaukee, WI; and ⁶New England Biolabs, Beverly, MA

Key Points

- We profiled platelet glycans by sequential mass spectrometry to characterize functional glycan epitopes and diverse isomeric structures.
- Sialylated structure abundance on N- and O-glycans decreases after room temperature storage.

Changes in surface glycan determinants, specifically sialic acid loss, determine platelet life span. The gradual loss of stored platelet quality is a complex process that fundamentally involves carbohydrate structures. Here, we applied lipophilic extraction and glycan release protocols to sequentially profile N- and O-linked glycans in freshly isolated and 7-day room temperature-stored platelet concentrates. Analytical methods including matrix assisted laser desorption/ionization time-of-flight mass spectrometry, tandem mass spectrometry, and liquid chromatography were used to obtain structural details of selected glycans and terminal epitopes. The fresh platelet repertoire of surface structures revealed diverse N-glycans, including high mannose structures, complex glycans with polylectosamine repeats, and glycans presenting blood group epitopes. The O-glycan repertoire largely comprised sialylated and fucosylated core-1 and core-2 structures. For both N- and O-linked glycans, we observed a loss in sialylated epitopes with a reciprocal increase in neutral structures as well as increased neuraminidase activity after platelet storage at room temperature. The data indicate that loss of sialylated glycans is associated with diminished platelet quality and untimely removal of platelets after storage.

Introduction

Platelets participate in hemostatic, inflammatory, and host defense reactions.¹ An adequate supply of platelets is essential to repair both continuously occurring vascular damage and to initiate thrombus formation after vascular injury. To ensure a steady platelet supply, humans produce and remove $\sim 10^{11}$ platelets daily, and the production rate can rise sharply under destruction conditions. Platelet production is tightly regulated to avoid spontaneous bleeding if counts are low as well as arterial occlusion and organ damage if counts are high.

The precise mechanisms regulating platelet clearance and production are under intense investigation.^{2,3} Recent studies have highlighted the role of glycan modifications on platelet surface glycoproteins in mediating clearance.^{4,5} Platelets presenting reduced $\alpha 2,3$ -linked sialic acid content owing to *Streptococcus pneumoniae* infection or in mice lacking the sialyltransferase ST3GalV are cleared by the hepatic Ashwell-Morell receptor (AMR) and macrophage galactose lectin (MGL).⁶⁻⁹ Loss of sialic

Submitted 18 January 2022; accepted 28 February 2023; prepublished online on *Blood Advances* First Edition 23 March 2023; final version published online 9 August 2023. <https://doi.org/10.1182/bloodadvances.2022007084>.

Data are available upon request from the corresponding author, Karin Hoffmeister (khoffmeister@versiti.org).

The full-text version of this article contains a data supplement.

© 2023 by The American Society of Hematology. Licensed under [Creative Commons Attribution-NonCommercial-NoDerivatives 4.0 International \(CC BY-NC-ND 4.0\)](https://creativecommons.org/licenses/by-nc-nd/4.0/), permitting only noncommercial, nonderivative use with attribution. All other rights reserved.

acid from platelets during their circulatory lifespan, termed *in vivo* aging, have been shown to induce platelet clearance also through the AMR and MGL.^{8,10,11}

Platelet transfusion is a widely used therapy to treat patients with thrombocytopenia. Because transfused cold-stored platelets are cleared rapidly from circulation, platelets for transfusion remain widely stored at room temperature (RT), which increases the risk of bacterial growth.^{12,13} We have demonstrated that 2 distinct pathways recognize asialylated- and agalactosylated glycans on platelet receptor GPIb α to remove refrigerated platelets in recipient's livers. First, hepatic asialoglycoprotein receptor AMR recognizes desialylated GPIb α .¹⁰ Second, $\alpha_M\beta_2$ integrins (Mac-1) on hepatic resident macrophages (Kupffer cells) selectively recognize irreversibly clustered β -N-acetylglucosamine (β -GlcNAc)-terminated glycans on GPIb α .^{14,15} Studies of glycan changes, particularly sialic acid loss during RT platelet storage, are debated, having shown contrasting results of both preservation and loss of epitope.¹⁶

Given the abundance of glycans on platelets, their role as ligand for lectin receptors, and debated RT storage-associated glycan changes, we performed a comprehensive analysis of the human platelet glycome on the day of isolation and 7 days after RT storage as platelet concentrates. It is noteworthy that platelet concentrates are not regularly used by blood banks. Glycoprotein glycans, specifically N- and O-linked glycans, were extracted for mass spectrometry analysis.¹⁷⁻¹⁹ Analytical methods such as matrix assisted laser desorption/ionization time-of-flight mass spectrometry (MALDI-TOF MS), tandem mass spectrometry (MS/MS or MSⁿ), and liquid chromatography (LC) were used in various combinations to confirm detailed glycan linkage and identity (Figure 1). When needed, synthetic standards were used as a comparison for the confirmation of observed structures.^{20,21} We observed an increase

in asialylated O-glycans and an increased abundance of neutral N-glycans after RT storage. In addition, we observed an increase in platelet surface neuraminidase activity in each donor following storage conditions. This finding suggests that glycan topology on platelets is, indeed, affected by storage and the reduced sialylation observed is induced by an increase in sialidase activity.

Materials and methods

Platelet collection and storage

Platelet concentrates from 3 nonpooled individual donors were purchased and stored at RT under standard blood banking conditions (22°C, shaking) for 7 days.²³ Platelet concentrates were prepared from single donor whole blood units and purchased from Research Blood Components (Watertown, MA). The blood was drawn, maintained, and processed at RT before shipment. Shipment occurred on the day of collection. The final platelet concentrates contained $6 \pm 0.7 \times 10^9$ in ~60 mL plasma with acid citrate dextose anticoagulant. Aliquots (3 mL of platelet rich plasma) were removed from the units under sterile conditions upon receipt (day 0) and after storage for 7 days (day 7) and processed for assays and mass spectrometry. The platelet concentrates were procured using the company's institutional review board, which allows only the release of deidentified material and did not include blood group information.

Platelet counts and preparation

Platelets were prepared from 3 platelet concentrates in unison by separating platelets from plasma by centrifugation at 900g for 5 minutes in the presence of 1 μ g/mL prostaglandin E₁ (PGE₁). Platelets were washed by centrifugation in buffer A (140 mM NaCl, 5 mM KCl, 12 mM trisodium citrate, 10 mM glucose, and 12.5 mM

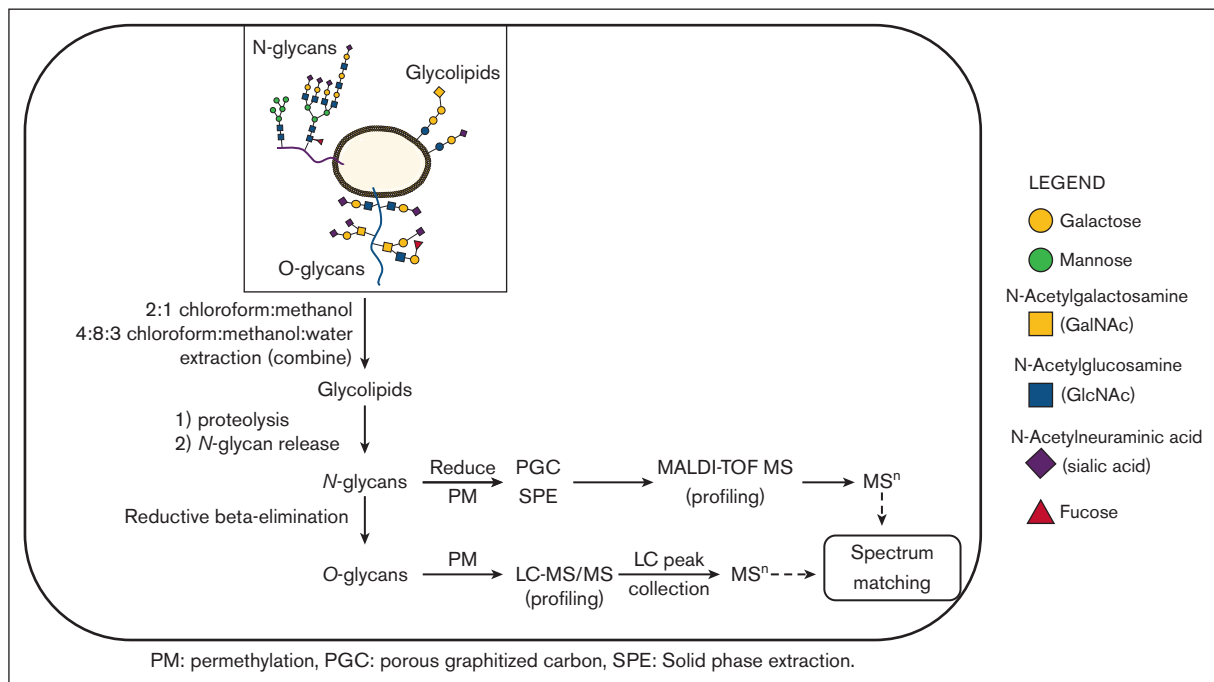


Figure 1. Outline of the workflow used to characterize human platelet glycoprotein glycome.²²

Table 1. Blood counts, platelet surface parameters, and recorded pH at day 0 and after 7 days of storage.

	Day 0 (PC)	Day 0 (isolated)	Day 7 (PC)	Day 7 (isolated)
Platelet count # ($\times 10^9/L$)	1507.6 \pm 373	1516 \pm 284	1403.3 \pm 377	1441 \pm 317
Platelet count ($\times 10^9/L$)	1710.7 \pm 66	1577.3 \pm 94	1580.0 \pm 17	1480.0 \pm 17
MPV # (fL)	10.5 \pm 0.9	10.3 \pm 0.9	10.3 \pm 0.95	9.8 \pm 0.65
WBC # ($\times 10^6/L$)	2.1 \pm 1.5	n.d.	1.7 \pm 1.5	n.d.
RBC # ($\times 10^9/L$)	1.4 \pm 0.26	n.d.	1.4 \pm 0.75	n.d.
CD42b (MFI)	63.3 \pm 12	51.9 \pm 20	61.6 \pm 20	57.8 \pm 10
CD61 (MFI)	58.3 \pm 14	48.7 \pm 18	63.1 \pm 18	53.8 \pm 18
P-Selectin (%)	5.7 \pm 1.1	5.0 \pm 1.7	7.6 \pm 1.7	7.0 \pm 2.8
NEU1 (MFI)	51.9 \pm 6.4	50.8 \pm 16	111.8 \pm 27***	111.0 \pm 14.3***
Annexin V (%)	2.2 \pm 1.4	1.29 \pm 2.1	5.6 \pm 2.6*	6.6 \pm 2.2*
RCA I (MFI)	401.4 \pm 176	382.3 \pm 166	714.1 \pm 264**	638.7 \pm 269**
ECL (MFI)	88.1 \pm 21	88.4 \pm 18	137.7 \pm 43**	131.1 \pm 28**
Con A (MFI)	47.9 \pm 4.4	47.4 \pm 4	149.6 \pm 27***	150.7 \pm 25***
pH	7.4 \pm 0.03	n.d.	7.3 \pm 0.05	n.d.

Platelet count indicated by #, WBC and RBC count were measured using an automated hematology analyzer (Sysmex). Platelet count was also measured using flow cytometry using reference beads. Platelet surface receptors CD42b (GPIIb) and CD61, the α -granule marker P-selectin, and NEU1 were measured by flow cytometry using specific mAb. PS exposure was measured by flow cytometry using annexin V. Surface terminal galactose was measured using RCA I and ECL lectins. % indicated positive events compared with control. Data are presented as mean \pm standard deviation from 7 donor platelet concentrates. The degree of significance is indicated * $P < .05$, ** $P < .01$, *** $P < .001$.

MPV, mean platelet volume; n.d., no data; PC, platelet concentrates; RBC, red blood cell; WBC, white blood cell.

sucrose, pH 6.0, supplemented with 1 μ g/mL PGE₁) for 10 minutes at RT and were suspended at 2×10^8 platelets/mL in buffer B (140 mM NaCl, 3 mM KCl, 0.5 mM MgCl₂, 5 mM NaHCO₃, 10 mM glucose, 10 mM HEPES, pH 7.4).

Complete blood counts were determined by Sysmex XP-300 automated hematology analyzer (Sysmex Corp). Isolated platelet counts were determined by Sysmex XP-300 automated hematology analyzer and by flow cytometry using 5.5 μ m diameter SPHERO rainbow beads as reference (Spherotech).^{13,24} Platelets were allowed to recover for 30 minutes at 37°C before analysis by flow cytometry and using automated hematology analyzer.

To eliminate glucose contamination for mass spectrometry, platelets were additionally washed once by centrifugation with phosphate saline buffer (PBS, 1 μ g/mL PGE₁) for mass spectrometric analysis. We did not detect white blood cells or red blood cells after platelet isolation and 30 minutes recovery using a hematology analyzer (Sysmex) (Table 1). For mass spectrometry, platelets were centrifuged at 900g for 5 minutes in the presence of 1 μ g/mL PGE₁ and platelet pellets collected after centrifugation were placed in liquid nitrogen immediately after 30 minutes recovery and stored at -80°C before preparation for mass spectrometry. On day 7, samples were collected and platelet pellets were prepared. The platelet pellets were transported on dry ice from the Harvard Medical School to the University of New Hampshire campus by the investigator. Total platelet pellets were prepared subsequently for mass spectrometry analysis as described below. Mass spectra shown here are exemplified using platelets from 3 single donors. Spectra were qualitatively comparable between individuals.

Antibodies

Anti-P-selectin-R-phycoerythrin (PE; CD62P, clone: AK4, indicates α -granule release) and PE isotype control antibody (Mouse IgG1 κ) were obtained from Becton Dickinson (Franklin Lakes, NJ).

Phycoerythrin-labeled annexin V (binds phosphatidylserine) and anti-human CD61 (integrin β_3) (RUU-PL7F12-FITC) were obtained from BD Biosciences. Anti-Neu1 IgG antibody and isotype control were obtained from Santa Cruz Biotechnology.

Flow cytometric analysis

Platelets were isolated, as described above, and stored at 37°C for 15 minutes, before fixation in BD Cytotfix (22°C, 20 min). Fixed platelets (1×10^6 cells/mL) were incubated for 1 hour with rabbit anti-Neu1 IgG antibody at RT and then washed with PBS in triplicate. The washed platelets were incubated for 30 minutes at RT with the appropriate antispecies secondary antibody Alexa Fluor 488 from Molecular Probes at a dilution of 1:500 followed by 3 washes in PBS. Other labeling of fixed, isolated platelets (1×10^6 cells/mL) was performed for 30 minutes at RT with fluorescently conjugated monoclonal antibodies (anti-CD61-FITC, anti-P-selectin-PE, anti-CD42b-FITC) and appropriate IgG controls.^{7,24,25}

For phosphatidylserine (PS) exposure, 1×10^7 nonfixed platelets were stained with phycoerythrin-labeled annexin V in 140mM NaCl, 10mM HEPES, and 2.5mM CaCl₂.²⁴ Platelets were analyzed on a FACSCalibur flow cytometer (BD Biosciences). Data were presented as either mean fluorescence intensity or the percentage of positive cells stained for P-selectin and annexin V. Mean fluorescence intensity is shown for fresh platelets before storage.

Measurement of platelet glycan exposure using lectins

Fresh platelets or platelets stored in plasma for 7 days at 22°C were collected by centrifugation at 830g for 5 minutes and suspended in buffer B at 1×10^7 /mL. Surface β -galactose were analyzed with 5 μ g/mL FITC-conjugated Erythrina cristagalli lectin (ECL) (Vector Laboratories) or 1 μ g/mL FITC-conjugated Ricinus communis agglutinin I (RCA I) or Concanavalin A (ConA) (Vector

Laboratories). Samples were incubated at RT for 20 minutes and analyzed by flow cytometry.

Sialidase activity

Platelets were assayed for sialidase activity with the use of 2'-(4-methylumbelliferyl)- α -D-*N*-acetylneuraminic acid (4-MU-NeuAc; BioSynth International). The 200 μ L reactions were completed at 37°C and initiated by adding 125 μ M 4-MU-NeuAc. Platelets (6×10^7) were used for each point, permeabilized with 2 μ L of 10 \times BD Perm/wash buffer (BD Biosciences) for total activity measurements and with 2 μ L 10 \times BD Wash Buffer to measure surface activity. Aliquots of 60 μ L of each reaction mixture were sampled, quenched with 180 μ L of 1M Na₂CO₃, and diluted with 60 μ L of reaction buffer. Background fluorescence was measured by incubating 60 μ L of platelets and substrate in separate reactions and sequentially adding them to 180 μ L of 1M Na₂CO₃. The reaction was recorded for 3 hours in triplicate.¹³

Mass spectrometry

Glycoconjugates were obtained from total platelet pellets using a sequential release protocol and then purified and analyzed as outlined (Figure 1). Total cell lysates were dried first by centrifugal evaporation and then sonicated in 3 mL of 2:1 chloroform:methanol for 3 hours at 40°C to extract glycosphingolipids (GSLs). A second GSL extraction step incorporated sonication with 4:8:3 chloroform:methanol:water (3 mL). The 2 GSL extracts were combined, redried, and then dissolved in chloroform and cleaned up by silica solid-phase extraction (SPE). Two SPE fractions were eluted using the following: (1) 9:1 acetone:methanol (neutral GSLs), and (2) methanol (acidic GSLs). The remaining protein pellets were then dried and washed 3 times with 80% aqueous acetone to remove any contaminating hexose polymers. To generate peptides and glycopeptides, the protein pellets were treated with 100 μ g each of trypsin (Sigma T0303) and chymotrypsin (Sigma C4129) in 50 mM ammonium bicarbonate at 37°C for 18 hours. The samples were then placed in a heating block at 100°C for 10 minutes to remove enzyme activity, and after cooling and a pH adjustment, the N-glycans were released with N-glycanase (ProZyme, Hayward, CA) at 37°C for 18 hours. The N-glycans were isolated by passage through a C18 SPE cartridge. Peptides, including O-linked glycopeptides, were then eluted from the SPE cartridge, as described elsewhere.²⁶ In the subsequent steps, the O-glycans were released using classical reductive β -elimination and cleaned up by a combination of ion exchange (Dowex AG50)²⁷ and C18 SPE. The N-glycans were reduced with borane-ammonia complex (10 mg/mL in ammonium hydroxide)²⁸ and further cleaned up by graphitized carbon SPE. Each glycoconjugate fraction (GSL, N-linked, O-linked) was then permethylated and profiled by MALDI-TOF-MS. For structural confirmation, selected glycans and glycan epitopes were disassembled by offline nanospray ion trap sequential mass spectrometry (NSI-IT-MSⁿ). O-glycans, obscured by background peaks at low mass, were additionally profiled using reverse phase (RP) LC-MS/MS²⁹ to overcome low mass background ions and improve quantitative interpretation. Each LC peak was then isolated for additional offline nanospray MSⁿ. Selected sialo- and fucosyl-moieties on N- and O-linked glycans were further identified by MSⁿ library spectral-matching, including comparison to synthetic standards. We did not include extended GSL characterization for this study.

Statistical analysis

All data are mean \pm standard error of the mean, unless otherwise indicated, because our experiments include imbalanced groups, whereby the precision of the mean effect depends directly on the sample size. We analyzed all numeric data for statistical significance with 1-way analysis of variance with Bonferroni correction for multiple comparisons with Prism software (GraphPad). We considered *P* values < .05 as statistically significant. Degrees of statistical significance are presented as ****P* < .001, ***P* < .01, and **P* < .05.

Results

Platelets have remarkable structural N-glycan diversity

In addition to abundant high-mannose N-glycans, particularly Man₅, platelets display diverse sialylated di-, tri-, and tetra-antennary complex N-glycans, including poly-lactosamine-bearing structures and antennal fucosylation (Figure 2, Table 2, supplemental Table 5).³⁰ MALDI-TOF was performed initially, followed by offline nanospray MS/MS to provide additional structural characterization information to global glycan compositions observed. For example, MSⁿ analysis of the sialylated di-lactosamine arm from compositional annotation was demonstrated (supplemental Figure 1). Likewise, the N-glycan composition with 1 core fucose and 1 antennary fucose yields in MS/MS (*m/z* 1217.9) the B-ion *m/z* 660; and subsequent MS³ of the ion *m/z* 660 and then MS⁴ of the fucosylated disaccharide fragment *m/z* 433 provide library-matching spectra indicating this structure contains an antennary H2 epitope (Fuc α 1-2Gal β 1-4GlcNAc)³¹ (supplemental Figure 2). We did not observe significant abundance of sialylated Lewis X (sLex) epitope presented by platelet N-glycans. After RT storage, we observed a decreased ratio in complex N-glycans with a concomitant increase in high mannose glycans (Figure 2). The high mass region (*m/z* 4000-7000) demonstrated reduced complex glycan signal after storage conditions, although the abundance changes in structures were minor in comparison with freshly isolated platelets (Figure 2). ConA lectin binds preferentially to terminal high mannose moieties. The increase in high mannose structures was corroborated by 2-fold increased ConA lectin binding to 7-day stored platelets compared with fresh controls (Table 1). Loss of sialic acid was corroborated by increased binding of terminal galactose binding lectins RCA I and ECL, increased sialidase activity and NEU1 surface presence, as detailed below (Table 1; supplemental Tables 1-4, Figure 4).

RT stored platelets lose sialylated O-glycans

Recent data show that appropriate O-linked glycosylation is intimately involved in human platelet biogenesis and function,³² prompting us to undertake further characterization of the platelet O-glycome. The O-linked glycan pools from human platelets were dominated by mono- and disialylated core-1 structures and asialo core-1 (the Thomsen-Friedenreich or TF-antigen). We also noted diverse fucosylated and sialylated core-2 type structures (Figure 3).³⁰ Each fresh vs 7-day stored platelet O-glycan pool was profiled by high-performance LC and the representative O-glycan peaks were isolated for further characterization by MSⁿ disassembly (Table 3). MSⁿ analysis of isomeric monofucosylated core-2

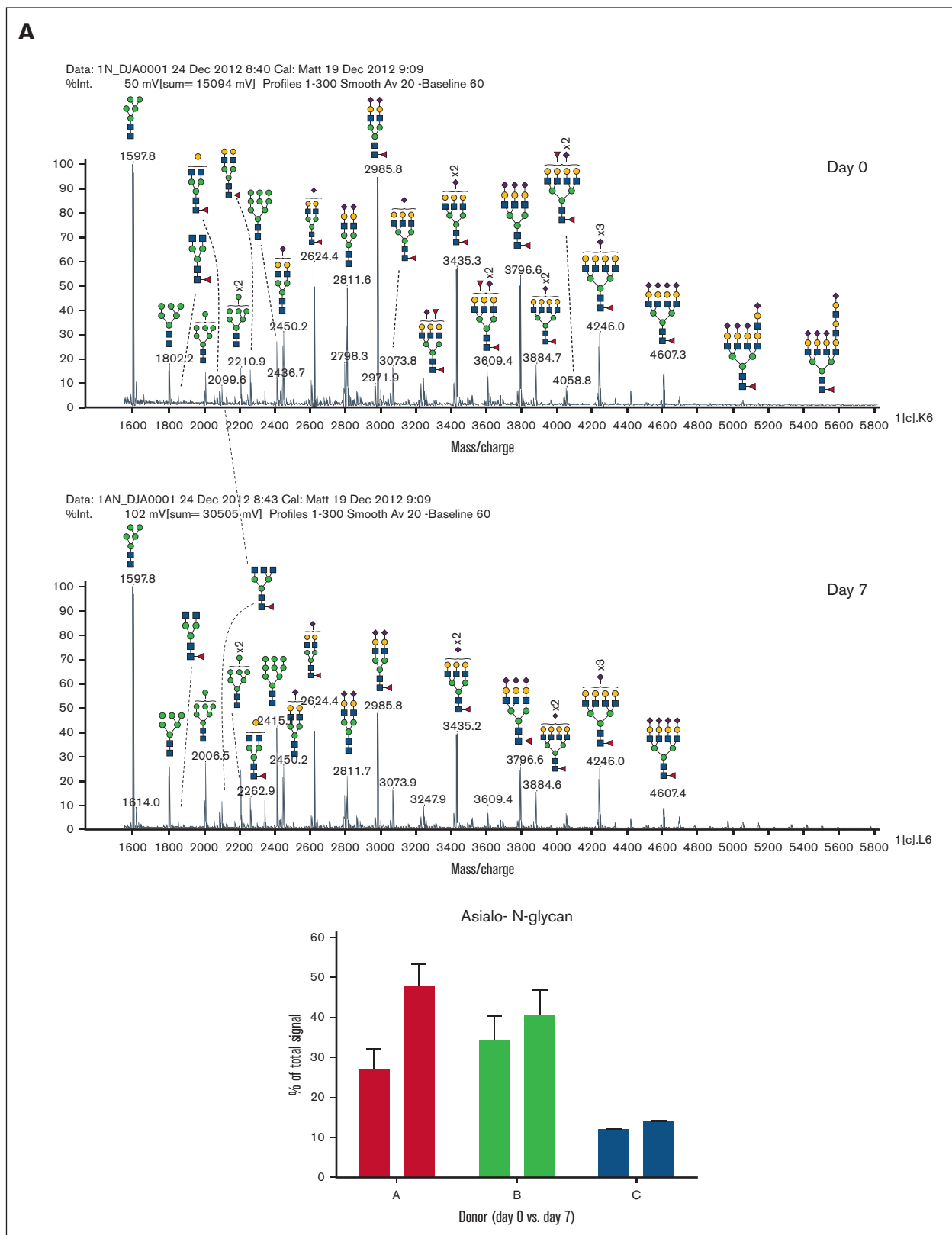


Figure 2. MALDI-TOF spectrum of N-glycans. (A) MALDI-TOF spectrum of the N-glycans released from human platelets (Table 2) on day 0 and upon RT storage at day 7 with asialo- N-glycan profile abundances summarized before and after storage for each donor. (B) High mass region for 1 donor on 0-day and 7-day platelet N-glycans showing diversity of lactosamine extensions.

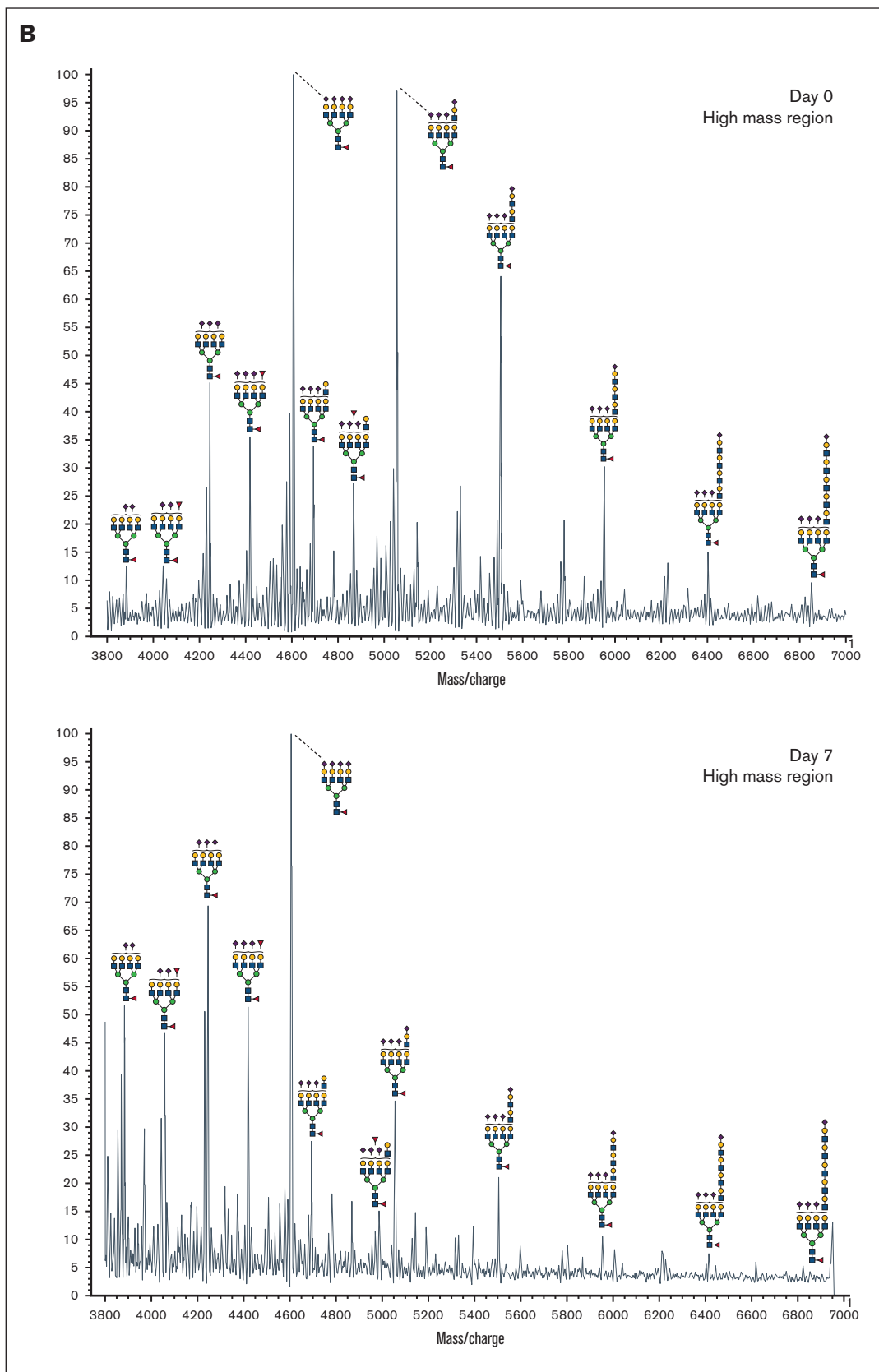


Figure 2 (continued)

Table 2. N-linked glycans detected in human platelets. N-linked glycans were analyzed by MALDI-TOF/MS

MALDI-TOF MS		Proposed Structure	MS ⁿ level
m/z (avg)	Theor Mass		
1597.2	1596.8		3
1801.5	1801.0		3
1853.4	1853.1		2
2005.3	2005.2		2
2098.8	2098.3		3
2128.8	2128.4		4
2210.6	2210.5		2
2262.3	2261.5		2
2414.3	2413.6		2
2449.3	2448.7		2
2623.6	2622.9		2
2810.6	2810.1		3
2984.7	2984.3		2
3073.1	3072.4		3
3247.3	3246.6		3
3434.3	3433.8		4
3608.6	3608.0		5
3796.0	3795.2		4
3884.0	3883.3		4
4058.0	4057.5		3
4245.5	4244.7		2
4419.4	4418.9		2
4606.9	4607.1		2
4695.0	4694.2		2
4868.8	4868.4		2
5055.9	5055.6		2
5943.8	5954.6		—
6403.3	6404.1		—
6852.9	6853.6		—

Proposed structures were shown as cartoon representations of glycans identified by MSⁿ analyses. The m/z value at which each glycan was detected is given as the sodiated ion of permethylated glycan. Theor Mass, theoretical mass.

O-glycans indicates that each displayed the H2 antigen on a separate arm of the core-2 motif, as identified by spectrum-matching (Figure 3; supplemental Figure 2). After the platelet storage at RT for 7 days, we observed a decrease in disialylated O-glycan with concomitant increase in neutral O-glycan structures in 3 different individuals. The changes observed regarding mono-sialylated structures were less consistent and decreased only in 1 donor (Figure 3; supplemental Table 6). Thus, the data demonstrate that O-glycans lose sialic acid moieties during storage. Loss of sialic acid was corroborated by increased binding of terminal galactose binding lectins RCA I and ECL (Table 1). However, these increases in lectin binding do not discriminate between loss of sialic acid on O- vs N-linked glycans.

RT storage increases platelet sialidase activity and NEU1 surface expression

The loss of sialic acids on N- and O-glycans observed after RT storage prompted us to measure sialidase activity and sialidase (NEU1) surface exposure. RT storage upregulated intracellular stores of NEU1 to the platelet surface, providing a feasible mechanism for desialylation of surface glycans. Enzyme activity assays showed that fresh platelets have low surface sialidase activity toward 4-MU-NeuAc, which increased by 2- to 3-fold after storage (Figure 4). This finding suggests that NEU1 is responsible, at least in part, for the increased sialidase activity exposed by storage. We measured different sialidase activities in fresh platelets and after storage between individuals, with data showing a ~20% to 50% upregulation of activity after 7 days depending on donor (Figure 4), suggesting that interindividual sialidase activity exist and contribute to loss of sialic acid during RT storage. We did not measure a significant change in CD42b or CD61 surface expression between fresh and stored platelets, although CD42b (GPIIb) expression decreased slightly after storage (Table 1). Approximately 5% of platelets had surface exposed P-selectin on day 0 which increased to 8% after 7-day RT storage. PS exposure was increased from 2% to 6% in stored platelets as measured by annexin V binding. Together, the data indicate that RT storage increased the following: (1) α-degranulation as indicated by P-selectin surface exposure, (2) NEU1 surface presence, and (3) sialidase activity that likely promotes loss of sialic acid.

Discussion

Decades-long research demonstrates that desialylation of blood components, including platelets, leads to their clearance from circulation.^{33,34} The expression of neuraminidase Neu1 that removes sialic acid from platelet glycoproteins, including GPIIb, causes desialylation of platelets during cold storage (4°C) followed by rewarming.¹³ Addition of a neuraminidase inhibitor to mouse platelets during refrigeration improves post-transfusion recovery and survival of refrigerated platelets. These inhibitory effects are similar to those on platelet desialylation and thrombocytopenia induced by GPIIb antiligand binding domain antibodies.³⁵⁻³⁷ Although the data show that loss of sialic acid promotes GPIIb

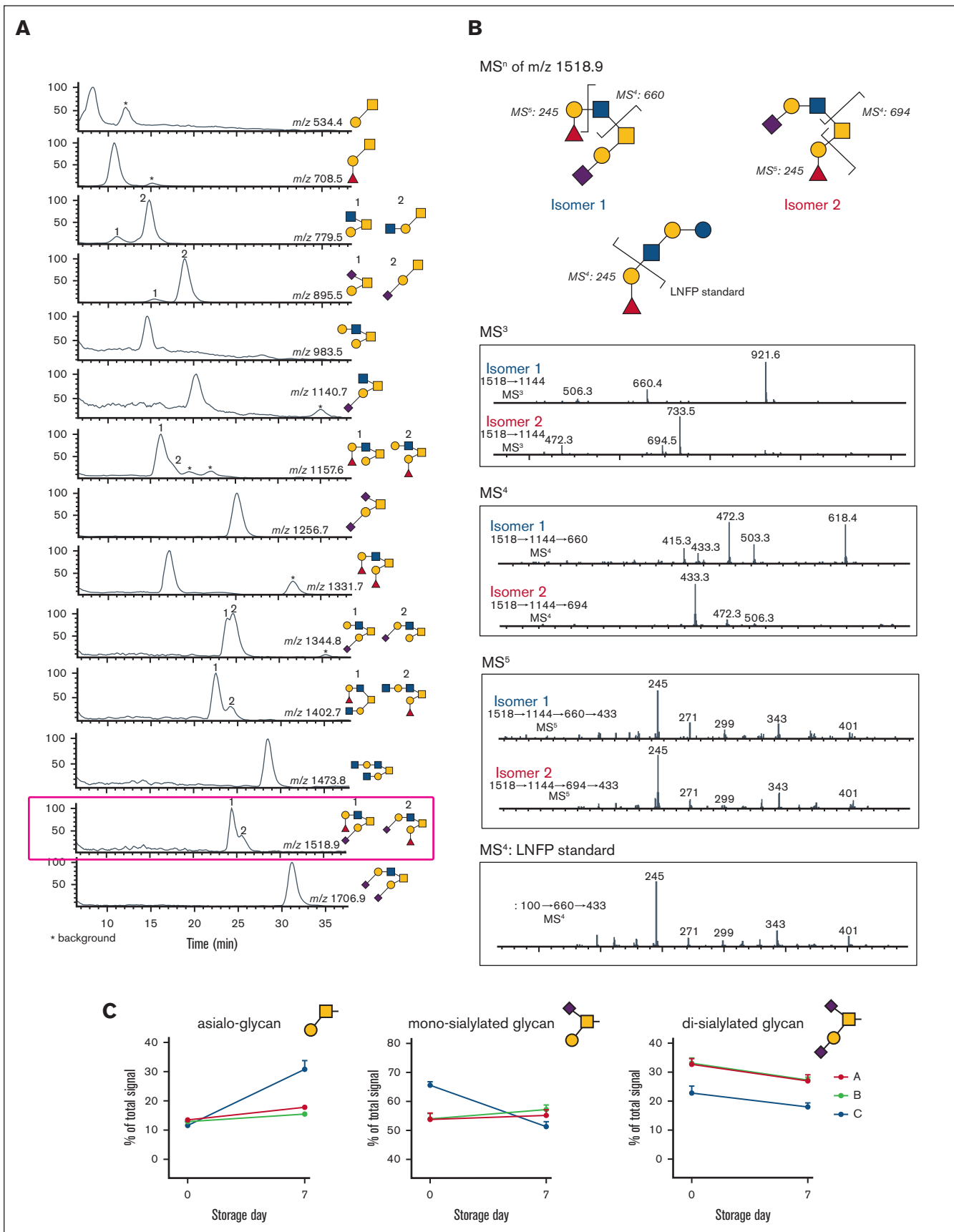


Figure 3.

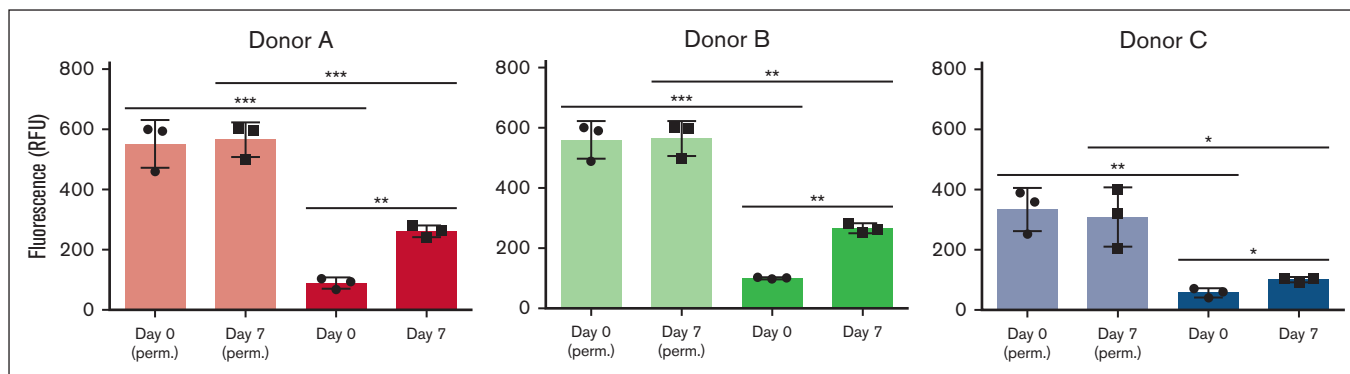


Figure 4. Sialidase activity associated with fresh and stored platelets from 3 individual donors. Total sialidase activity in platelets was measured in nonpermeabilized RT platelets at day 0 and day 7 and in permeabilized RT platelets ($n = 3$). Total sialidase activity in platelets was measured in day-0 permeabilized RT platelets. The amount of 4-methylumbelliferone released in quenched reaction mixtures was measured in 96-well Microfluor-1 Black plates on a Spectra MAX GEMINI EM Microplate Spectrofluorometer (molecular devices) with excitation, emission, and cutoff wavelengths of 355, 460, and 455 nm, respectively. Background fluorescence was subtracted from each data point. Sialidase activity recorded at 3 hours is shown. The degree of significance is indicated as $*P < .05$, $**P < .01$.

cleavage and negatively impacts platelet lifespan after refrigerated platelet storage, the effect of neuraminidase inhibition on cold-stored human platelets has yet to be explored.³⁸⁻⁴⁰

Studies on whether RT storage can lead to similar changes in sialylation yielded mixed results. In an early study, Soslau et al showed that human platelets lost 30% and 70% of sialic acid during the first 3 and 7 days of incubation at RT, respectively.⁴¹ Cho et al also showed that platelet concentrates lose sialic acid content upon storage.¹⁶ Conversely, Rijkers et al did not identify changes in sialic acid levels or GPIIb α and GPV loss after human platelet storage at RT by flow cytometry analysis using lectins and monoclonal antibodies, respectively.⁴² These contradictory data may be attributed to different storage conditions, such as apheresis platelets and single donor platelet concentrates with and without platelet additive solutions. Methodologies applied to measure the loss of sialic acid and differences in sialic acid content and expression between mouse and human platelets can also contribute to the differences in observed sialic acid loss. Our glycomic analysis measured changes in glycan topology using total platelet lysates, whereas other studies measured terminal galactose structures on platelet surface using lectins (ECA and RCA I).⁴³ It is possible that lectin binding fails to detect loss of sialic acid on O-glycans, which are notoriously difficult to study owing to high glycan density and accessibility for analysis. More detailed O-glycan characterization is needed using proteases that allow better accessibility to O-glycans, specific in mucin-rich regions.⁴⁴ Thus, the contribution of sialic acid loss and receptor proteolysis during RT platelet storage has been demonstrated but remains debated. A limitation of our study was the potential contamination of platelets by plasma protein contaminants, possibly trapped in the open canalicular system.


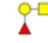



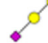













The abundance of asialo-N-glycans measured on day 0 platelets differ between the 3 individuals analyzed. The changes noted

between fresh vs 7-day stored platelets using MALDI-TOF showed that the degree of sialic acid loss also varies between 3 individuals (supplemental Tables 5 and 6). Sialidase activity showed interindividual differences on day 0, when the lowest measured sialidase activity coincides with a low abundance of asialo-N-glycans (supplemental Tables 2 and 4). After day 7, the increase in sialidase activity coincides with N-glycan sialic acid loss. The sample variation suggests that although losses are generalizable, interindividual differences exist in the extent of sialic acid loss and sialidase activity (Figure 4). Although the analyzed sample size is small ($n = 7$), the presented data point to interindividual differences in platelet sialidase activity, NEU1 surface expression, and sialic acid content between individuals in fresh and after RT storage, which needs further investigation with an increased cohort of donors. Of note, total permeabilized sialidase activity was comparable between day 0 and day 7 platelets (Figure 4). Hence, the increase in sialidase activity on platelets points to surface exposure of sialidases, perhaps caused by translocation of secretory lysosomal enzymes. Our data did not show marked differences in other activation markers, such as P-selectin or PS exposure between the individuals. It is tempting to speculate that an individual's lysosomal activity and sialidase activity affect the interindividual glycan topology differences, thereby contributing to accelerated platelet clearance after transfusion. As mass spectrometry advances in automatization, more comprehensive studies will be possible, specifically applying glycoproteomic analyses of platelets.

Our data show platelet branched N-glycans bear an elongated disaccharide structure of LacNAc [(Gal β 1-4GlcNAc) $_1$] $_x$ (m/z 6852.9, 6403.3, 5943.8, 5055.9, 4868.8, 4695.0) known as polylactosamine (polyLacNAc). PolyLacNAc is synthesized by the alternative action of β 1,4-galactosyltransferases (β 4GalT1) and a β 1,3-N-acetylglucosaminyltransferase (β 3GnT). Our recent work indicates that absence of β 4GalT1 in megakaryocytes impairs

Figure 3. MALDI-TOF spectrum of N-glycans. (A) LC-MS/MS of O-glycans released from human platelets, showing extracted ion chromatogram. The peaks were collected, and each structure was confirmed by MSⁿ (Table 3). (B) MSⁿ disassembly of isomeric fucosylated O-glycans isolated by high-performance LC (m/z 1518.9) with spectral match of Fuc(α 1,2)Gal, from the standard LNFP-I (lacto-N-fucopentaose I) in MSⁿ. (C) Quantification of released O-glycans, classified by sialylation status (neutral/asialo-, monosialylated, or disialylated) was performed by extracted ion chromatographs. Example structures are depicted, with the conclusive list of structures quantified found in Table 3.

Table 3. O-linked glycans detected in human platelets. O-glycans were analyzed by MALDI-TOF/MS and the isobaric structures of O-linked glycans were identified by LC-MS/MS

RT	m/z	Structure	MS ⁿ level
8.2	534.4		2
10.7	708.5		3
11.0	779.5		3
14.6	779.5		3
17.2	895.5		3
21.2	895.5		3
14.6	983.5		4
20.9	1140.7		3
16.1	1157.6		5
17.1	1157.6		5
25.1	1256.7		4
17.0	1331.7		5
24.0	1344.8		5
24.5	1344.8		5
22.4	1402.7		5
24.2	1402.7		5
28.4	1473.8		5
24.4	1518.9		6
25.5	1518.9		6

The m/z value at which each glycan was detected is given as the sodiated ion of permethylated glycan. RT, retention time.

mouse thrombopoiesis in vivo and in vitro indicating that lactosamine and polyLacNAc synthesis is an integral part.⁴⁵ Here, polyLacNAc structure abundance is not significantly changed after storage, whereas relative amounts of polyLacNAc in the total glycome is low (Figure 2). It is tempting to speculate that polyLacNAc N-glycans are not affected by storage but are essential in thrombopoiesis. N-glycan analysis also revealed a low abundance of sLex, a canonical selectin ligand. Mouse model knockouts of sLex ligands, specifically the selectin family, do not display any thrombocytopenia or bleeding phenotype, thus the role and expression of sLex epitopes needs further investigation.⁴⁶ Lastly, the platelet N-glycan repertoire also had large amounts of high mannose structures on nonstored platelets (m/z 1597.2, 1801.5, 2005.3,

2210.6, 2414.3), typically associated with cell secretory systems. High mannose surface expression correlated with ConA lectin binding that increased after storage in all 7 individuals. In mammalian cells, high mannose structures are precursors of complex glycans and are located on the endoplasmic reticulum and cis-Golgi compartments. A recent report suggests that the formation of the demarcation membrane system (DMS), a significant step during megakaryocyte development, depends on the secretory pathway.⁴⁷ These observations suggest that glycans associated with the secretory pathway may contribute to platelet biogenesis.

In addition to N-glycans, we used LC-MSⁿ method to detect a quantifiable loss of sialylated O-glycans after storage of platelets at RT (Figure 3). In agreement with previous studies of human serum, our analysis shows that platelet glycans comprise largely core-1 and core-2 O-glycans.⁴⁸ A recent study identified the O-glycan landscape on platelet glycoproteins, in which GPIb α contained the largest amount of sites.⁴⁹ Platelet GPIb α is highly glycosylated, accounting for as much as 60% of its molecular weight.⁵⁰ It is tempting to speculate that loss of O-glycan sialic acid occurs predominantly on platelet GPIb α , perhaps leading to decreased GPIb α surface expression after storage. More detailed O-glycoproteomic/glycomics and analysis of the proteolytic activity in stored platelets will be required to determine this conclusively. Blood group antigens were detected in both N- and O-glycans. In red blood cells, blood group antigens are found primarily on 2 glycoproteins, band 3 and band 4.5, with a small portion found on glycolipids.⁵¹ Whether the distribution of blood group antigens on platelets is limited to a few glycoproteins requires extended glycoproteomic analysis.

A limitation of this study is the analysis of glycans after pelleting and freezing of platelets. Platelet freezing causes a decrease in glycoprotein expression, including GPIb α and GPIIb.⁵² A decrease in peanut agglutinin (PNA) lectin binding following platelet cryopreservation has been reported.⁵³ PNA has a specificity for Gal β 1-3GalNAc (core-1 or the TF-antigen) moieties, but this binding is inhibited upon sialylation. A decrease in PNA binding after platelet cryopreservation could indicate an increase in sialylation or loss of the TF-antigen; however, we did not perform lectin binding analysis after platelet freezing for mass spectrometry. Our glycomics analysis indicates that core-1 O-glycan abundance increased for 2 of the donors analyzed. Thus, it is possible that freezing platelets for mass spectrometry affects the glycan expression levels, but our study is limited to lectin binding data to platelet before preparation for mass spectrometry.

In summary, we provided a comprehensive analysis of the human platelet N- and O-glycome. Platelet N-glycans feature high-mannose structures, branched complex glycans, and polyLacNAc extensions. Platelet O-glycans largely comprises core-1 and core-2 structures. We compared platelet glycome alterations upon 7 days of RT storage and observed a decrease in sialylation in both N- and O-glycans. The extent of this sialic acid loss differed between individuals. We also observed differences in sialidase activity and NEU1 expression between individuals, which coincide with the loss of sialic acid.⁵⁴ It is important to note that we used platelet concentrates and not the routinely used apheresis platelets in this study.^{55,56} Thus, the data may not be completely representative of glycan topology change in platelets procured by apheresis.

However, the data here serve as a foundation to understanding the diverse role of glycans in platelets during storage.

Acknowledgments

This work was supported by US National Institutes of Health, National Heart, Lung, and Blood Institute grants R01 HL089224 (K.M.H.), P01 HL107146 (project director: K.M.H.), and K12 HL141954 (program director: K.M.H.).

Authorship

Contribution: A.J.S.H., K.E.R., M.M.L.-S., K.A., and R.G. performed experiments, analyzed results, and created the figures; A.J.S.H. and

K.M.H. designed the research; M.M.L.-S., A.J.S.H., and K.M.H. wrote the manuscript; and D.J.A. compiled the supplemental figures.

Conflict-of-interest disclosure: K.M.H. and M.M.L.-S. have received consulting fees from Pfizer. The remaining authors declare no competing financial interests.

ORCID profiles: K.A., [0000-0003-0029-4291](#); K.M.H., [0000-0001-6526-7919](#).

Correspondence: Karin Hoffmeister, Translational Glycomics Center, Versiti Blood Research Institute, Milwaukee, WI 53226; email: khoffmeister@versiti.org.

References

1. Gremmel T, Frelinger AL 3rd, Michelson AD. Platelet physiology. *Semin Thromb Hemost.* 2016;42(3):191-204.
2. Shrivastava M. The platelet storage lesion. *Transfus Apher Sci.* 2009;41(2):105-113.
3. Ng MSY, Tung JP, Fraser JF. Platelet storage lesions: what more do we know now? *Transfus Med Rev.* 2018;32(3):144-154.
4. Toonstra C, Hu Y, Zhang H. Deciphering the roles of N-glycans on collagen-platelet interactions. *J Proteome Res.* 2019;18(6):2467-2477.
5. Korrel SA, Clemetson KJ, van Halbeek H, Kamerling JP, Sixma JJ, Vliegthart JF. Identification of a tetrasialylated monofucosylated tetraantennary N-linked carbohydrate chain in human platelet glycoprotein. *FEBS Lett.* 1988;228(2):321-326.
6. Sorensen AL, Rumjantseva V, Nayeb-Hashemi S, et al. Role of sialic acid for platelet life span: exposure of beta-galactose results in the rapid clearance of platelets from the circulation by asialoglycoprotein receptor-expressing liver macrophages and hepatocytes. *Blood.* 2009;114(8):1645-1654.
7. Grozovsky R, Begonja AJ, Liu K, et al. The Ashwell-Morell receptor regulates hepatic thrombopoietin production via JAK2-STAT3 signaling. *Nat Med.* 2015;21(1):47-54.
8. Grewal PK, Uchiyama S, Ditto D, et al. The Ashwell receptor mitigates the lethal coagulopathy of sepsis. *Nat Med.* 2008;14(6):648-655.
9. Nimrichter L, Burdick MM, Aoki K, et al. E-selectin receptors on human leukocytes. *Blood.* 2008;112(9):3744-3752.
10. Rumjantseva V, Grewal PK, Wandall HH, et al. Dual roles for hepatic lectin receptors in the clearance of chilled platelets. *Nat Med.* 2009;15(11):1273-1280.
11. Deppermann C, Kratochvil RM, Peiseler M, et al. Macrophage galactose lectin is critical for Kupffer cells to clear aged platelets. *J Exp Med.* 2020;217(4):e20190723.
12. Hoffmeister KM, Felbinger TW, Falet H, et al. The clearance mechanism of chilled blood platelets. *Cell.* 2003;112(1):87-97.
13. Jansen AJG, Josefsson EC, Rumjantseva V, et al. Desialylation accelerates platelet clearance after refrigeration and initiates GPIIb/alpha metalloproteinase-mediated cleavage in mice. *Blood.* 2012;119(5):1263-1273.
14. Josefsson EC, Gebhard HH, Stossel TP, Hartwig JH, Hoffmeister KM. The macrophage alphaMbeta2 integrin alphaM lectin domain mediates the phagocytosis of chilled platelets. *J Biol Chem.* 2005;280(18):18025-18032.
15. Badlou BA, Spierenburg G, Ulrichs H, Deckmyn H, Smid WM, Akkerman JWN. Role of glycoprotein Iba1 in phagocytosis of platelets by macrophages. *Transfusion.* 2006;46(12):2090-2099.
16. Cho J, Kim H, Song J, et al. Platelet storage induces accelerated desialylation of platelets and increases hepatic thrombopoietin production. *J Transl Med.* 2018;16(1):199.
17. Rosenbalm KE, Tiemeyer M, Wells L, Aoki K, Zhao P. Glycomics-informed glycoproteomic analysis of site-specific glycosylation for SARS-CoV-2 spike protein. *STAR Protoc.* 2020;1(3):100214.
18. Huang YF, Aoki K, Akase S, et al. Global mapping of glycosylation pathways in human-derived cells. *Dev Cell.* 2021;56(8):1195-1209.e7.
19. Nairn AV, Aoki K, dela Rosa M, et al. Regulation of glycan structures in murine embryonic stem cells: combined transcript profiling of glycan-related genes and glycan structural analysis. *J Biol Chem.* 2012;287(45):37835-37856.
20. Aoki K, Heaps AD, Strauss KA, Tiemeyer M. Mass spectrometric quantification of plasma glycosphingolipids in human GM3 ganglioside deficiency. *Clin Mass Spectrom.* 2019;14 Pt B:106-114.
21. Mehta N, Porterfield M, Struwe WB, et al. Mass spectrometric quantification of N-linked glycans by reference to exogenous standards. *J Proteome Res.* 2016;15(9):2969-2980.
22. Neelamegham S, Aoki-Kinoshita K, Bolton E, et al. Updates to the Symbol Nomenclature for Glycans guidelines. *Glycobiology.* Aug 20 2019;29(9):620-624.

23. Singh RP, Marwaha N, Malhotra P, Dash S. Quality assessment of platelet concentrates prepared by platelet rich plasma-platelet concentrate, buffy coat poor-platelet concentrate (BC-PC) and apheresis-PC methods. *Asian J Transfus Sci.* 2009;3(2):86-94.
24. Jurak Begonja A, Hoffmeister KM, Hartwig JH, Falet H. FlnA-null megakaryocytes prematurely release large and fragile platelets that circulate poorly. *Blood.* 2011;118(8):2285-2295.
25. Alugupalli KR, Michelson AD, Barnard MR, Leong JM. Serial determinations of platelet counts in mice by flow cytometry. *Thromb Haemost.* 2001;86(2):668-671.
26. Babu P, North SJ, Jang-Lee J, et al. Structural characterisation of neutrophil glycans by ultra sensitive mass spectrometric glycomics methodology. *Glycoconj J.* 2009;26(8):975-986.
27. Carlson DM. Oligosaccharides isolated from pig submaxillary mucin. *J Biol Chem.* 1966;241(12):2984-2986.
28. Huang Y, Konse T, Mechref Y, Novotny MV. Matrix-assisted laser desorption/ionization mass spectrometry compatible beta-elimination of O-linked oligosaccharides. *Rapid Commun Mass Spectrom.* 2002;16(12):1199-1204.
29. Hanisch FG, Muller S. Analysis of methylated O-glycan alditols by reversed-phase NanoLC coupled CAD-ESI mass spectrometry. *Methods Mol Biol.* 2009;534:107-115.
30. Butta NV, Haslam SM, Dell A, et al. Glycomic characterization of platelets from patients with immune thrombocytopenia. *Blood.* 2021;138(Supplement 1):3158.
31. Ashline DJ, Hanneman AJS, Zhang H, Reinhold VN. Structural documentation of glycan epitopes: sequential mass spectrometry and spectral matching. *J Am Soc Mass Spectrom.* 2014;25(3):444-453.
32. Wang Y, Jobe SM, Ding X, et al. Platelet biogenesis and functions require correct protein O-glycosylation. *Proc Natl Acad Sci U S A.* 2012;109(40):16143-16148.
33. Aminoff D, Bell WC, VorderBruegge WG. Cell surface carbohydrate recognition and the viability of erythrocytes in circulation. *Prog Clin Biol Res.* 1978;23:569-581.
34. Marikovsky Y, Elazar E, Danon D. Rabbit erythrocyte survival following diminished sialic acid and ATP depletion. *Mech Ageing Dev.* 1977;6(3):233-240.
35. Li J, van der Wal DE, Zhu G, et al. Desialylation is a mechanism of Fc-independent platelet clearance and a therapeutic target in immune thrombocytopenia. *Nat Commun.* 2015;6:7737.
36. Bigot P, Auffret M, Gautier S, Weinborn M, Ettahar NK, Coupe P. Unexpected platelets elevation in a patient with idiopathic thrombocytopenia treated with oseltamivir for influenza infection. *Fundam Clin Pharmacol.* 2016;30(5):483-485.
37. Revilla N, Corral J, Minano A, et al. Multirefractory primary immune thrombocytopenia; targeting the decreased sialic acid content. *Platelets.* 2019;30(6):743-751.
38. Hollenhorst MA, Tiemeyer KH, Mahoney KE, et al. Comprehensive analysis of platelet glycoprotein Iba glycosylation. *bioRxiv.* 2022.
39. Jansen AJG, Peng J, Zhao HG, Hou M, Ni H. Sialidase inhibition to increase platelet counts: a new treatment option for thrombocytopenia. *Am J Hematol.* 2015;90(5):E94-E95.
40. Shaim H, McCaffrey P, Trieu JA, DeAnda A, Yates SG. Evaluating the effects of oseltamivir phosphate on platelet counts: a retrospective review. *Platelets.* 2020;31(8):1080-1084.
41. Soslau G, Giles J. The loss of sialic acid and its prevention in stored human platelets. *Thromb Res.* 1982;26(6):443-455.
42. Rijkers M, van der Meer PF, Bontekoe IJ, et al. Evaluation of the role of the GPIIb-IX-V receptor complex in development of the platelet storage lesion. *Vox Sang.* 2016;111(3):247-256.
43. Lasne D, Pascreau T, Darame S, et al. Measuring beta-galactose exposure on platelets: Standardization and healthy reference values. *Res Pract Thromb Haemost.* 2020;4(5):813-822.
44. Malaker SA, Pedram K, Ferracane MJ, et al. The mucin-selective protease StcE enables molecular and functional analysis of human cancer-associated mucins. *Proc Natl Acad Sci U S A.* 2019;116(15):7278-7287.
45. Giannini S, Lee-Sundlov MM, Rivadeneyra L, et al. beta4GALT1 controls beta1 integrin function to govern thrombopoiesis and hematopoietic stem cell homeostasis. *Nat Commun.* 2020;11(1):356.
46. Frenette PS, Mayadas TN, Rayburn H, Hynes RO, Wagner DD. Susceptibility to infection and altered hematopoiesis in mice deficient in both P- and E-selectins. *Cell.* 1996;84(4):563-574.
47. Eckly A, Heijnen H, Pertuy F, et al. Biogenesis of the demarcation membrane system (DMS) in megakaryocytes. *Blood.* 2014;123(6):921-930.
48. Yabu M, Korekane H, Miyamoto Y. Precise structural analysis of O-linked oligosaccharides in human serum. *Glycobiology.* 2014;24(6):542-553.
49. King SL, Joshi HJ, Schjoldager KT, et al. Characterizing the O-glycosylation landscape of human plasma, platelets, and endothelial cells. *Blood Adv.* 2017;1(7):429-442.
50. Tsuji T, Tsunehisa S, Watanabe Y, Yamamoto K, Tohyama H, Osawa T. The carbohydrate moiety of human platelet glycolalicin. *J Biol Chem.* 1983;258(10):6335-6339.
51. Stanley P, Cummings RD. Structures Common to Different Glycans. In: Varki A, Cummings RD, Esko JD, et al, eds. *Essentials of Glycobiology.* Cold Spring Harbor Press; 2009:175-198.
52. Wood B, Padula MP, Marks DC, Johnson L. The immune potential of ex vivo stored platelets: a review. *Vox Sang.* 2021;116(5):477-488.

53. Johnson L, Tan S, Wood B, Davis A, Marks DC. Refrigeration and cryopreservation of platelets differentially affect platelet metabolism and function: a comparison with conventional platelet storage conditions. *Transfusion*. 2016;56(7):1807-1818.
54. van der Wal DE, Davis AM, Mach M, Marks DC. The role of neuraminidase 1 and 2 in glycoprotein Ibalph-mediated integrin alphaIIb beta3 activation. *Haematologica*. 2020;105(4):1081-1094.
55. Curvers J, van Pampus ECM, Feijge MAH, Rombout-Sestriekova E, Giesen PLA, Heemskerk JWM. Decreased responsiveness and development of activation markers of PLTs stored in plasma. *Transfusion*. 2004;44(1):49-58.
56. van der Wal DE, Davis AM, Marks DC. Donor citrate reactions influence the phenotype of apheresis platelets following storage. *Transfusion*. 2022;62(2):273-278.